A Letters Journal Exploring the Frontiers of Physics

June 2007

EPL, **78** (2007) 57003
doi: 10.1209/0295-5075/78/57003

www.epljournal.org

Evolution of a symmetry gap and synergetic quantum well states in ultrathin Ag films on Au(111) substrates

Li Huang[1,2], X. G. Gong[1], E. Gergert[3], F. Forster[3], A. Bendounan[3], F. Reinert[3] and Zhenyu Zhang[2,4]

[1] *Surface Physics Laboratory and Department of Physics, Fudan University, Shanghai 200433, P.R. China*
[2] *Materials Science and Technology Division, Oak Ridge National Laboratory, Oak Ridge, TN 37831, USA*
[3] *Experimentelle Physik II, Universität Würzburg, Würzburg D-97074, Germany*
[4] *Department of Physics and Astronomy, University of Tennessee, Knoxville, 37996, USA*

received 19 December 2006; accepted in final form 18 April 2007
published online 16 May 2007

PACS 71.15.Nc – Total energy and cohesive energy calculations
PACS 79.60.Dp – Adsorbed layers and thin films
PACS 79.60.-i – Photoemission and photoelectron spectra

Abstract – Using first-principles calculations within density functional theory (DFT) and high-resolution angle-resolved photoemission spectroscopy (ARPES), we carry out a comprehensive study of how a symmetry gap around the Fermi level develops towards its bulk value as the thickness of Ag films grown on an Au(111) substrate increases. We show that, contrary to prevailing assumptions, the symmetry gap in ultrathin Ag films can be substantially wider than the gap of the Au substrate along the [111] direction. As a result, the first and second quantum well states (QWS) are confined within the Ag films only when the film reaches a certain thickness. We further show that, when ultrathin Au films are grown on Ag(111) slabs of comparable thicknesses, synergetic QWS spanning across the whole (Au+Ag) systems are established.

The existence or absence of an energy gap around the Fermi level of a crystalline solid is of fundamental importance, determining many characteristic properties of the material. For a given material, the energy gap can be dependent on the orientation, dimensionality, and size of the system, among other factors. As an example in the zero-dimensional regime, the energy gaps of clusters are usually larger than those of the corresponding bulk materials, and it remains fundamentally intriguing to understand precisely how the energy gap evolves towards the bulk value as the cluster size increases [1,2]. In the three-dimensional regime, symmetry gaps along certain direction of the Brillouin zone can appear even for metals that do not have true energy gaps. Such local symmetry gaps can serve as potential energy barriers to confine electrons moving along these directions, leading to the formation of localized electronic states of surfaces and thin films, such as the surface and image states within the inverted *sp*-band gaps of the noble metal (111) surfaces [3–5].

More recently, considerable attention [6–9] has been paid to electron motion in ultrathin metal films on metallic [10–18], semiconducting [19–23], or quasi-crystalline substrates [24]. For such systems, there may exist a mismatch in the band gaps along the direction normal to the film, reflecting the electrons moving in the film towards the metal-substrate interface. This reflection, together with the reflection at the metal-vacuum interface on the other side, results in the formation of standing waves, or quantum well states (QWS), in the metal film. One first example exhibiting QWS in metal films on metal substrates was Ag on Au(111), observed in photoemission measurements [8,10]. Here, one or more QWS were observed when the Ag film thickness reached 10 monolayers (ML) or thicker. In contrast, when Ag films were grown on Fe(100) [15] or V(100) substrates [6,16], QWS were already observed even for the thinnest films of 1 or 2 ML. Precisely what leads to the contrasting behaviors of Ag on the different substrates remains elusive. In particular, the quantum size effect (QSE), which is ultimately responsible for the appearance of QWS, is supposed to be more pronounced for thinner films, yet for Ag on Au(111) no QWS were observed in the first few atomic layers [8,10]. Furthermore, essentially all existing theoretical interpretations have been based on the misalignment picture of the bandgaps of *bulk* Ag and Au, explicitly invoking a constant value of ~ 0.33 eV for the Ag valence-band edge in the Γ-L direction [8,10,14].

In this letter, we present a systematic theoretical and experimental study of how a symmetry gap around the Fermi level evolves as a metal film grown on a metal substrate increases its thickness layer by layer, using Ag/Au(111) as a prototype system. By a comparison of density functional theory (DFT) calculation results with high-resolution angle-resolved photoemission spectroscopy (ARPES), we show that the symmetry gap in ultrathin Ag films can be substantially wider than either the symmetry gap of bulk Ag or that of the Au substrate. Consequently, the first bound state can be defined within the Ag films only when the Ag film thickness reaches about 10 ML, corresponding to the case where the Ag symmetry gap becomes distinctly narrower than that of Au. When the thickness increases beyond 18 ML, a second bound state falls into the gap region of the substrate, thereby confining the second QWS in the Ag films. We further show that, when ultrathin Au films are grown on Ag(111) overlayers of comparable thicknesses, synergetic QWS spanning across the whole (Au+Ag) systems are established, owing to the isovalency and negligible lattice mismatch between the two elements. These results help to rationalize the results of high-resolution photoemission measurements on a quantitative level.

Our calculations are carried out using the VASP code [25] based on DFT with ultrasoft pseudopotentials [26] and plane-wave basis sets. The exchange-correlation effects are described within the generalized gradient approximation [27]. The energy cutoff for plane waves is 29 Ry. Relativistic effects are included at the scalar level, with the Ag and Au d orbitals included as valence states in generation of the pseudopotentials. The calculated equilibrium lattice constants for bulk Au and Ag are 4.18 Å and 4.17 Å, respectively, in good agreement with the experimental values (4.08 Å for Au and 4.09 Å for Ag). For Ag/Au(111), the systems are modeled by periodic slabs, which contain a vacuum spacing of 25 Å, an Au substrate of at least 25 ML, and Ag films of desired thicknesses. The tiny lattice mismatch of $\sim 0.2\%$ between Au and Ag is ignored by using the Au lattice constant for both elements. The Brillouin zone sampling is performed using a $20 \times 20 \times 1$ Monkhorst-Pack k-point mesh [28]. In each case, the positions of the substrate atoms are fixed, while the interlayer spacings in the Ag overlayers are relaxed until the largest residual forces become less than 0.02 eV/Å, and the total energy is converged to the order of 10^{-4} eV. Tests have been performed to make sure that all the results are fully converged with respect to the energy cutoff, system size, k-point sampling. We have also checked the relaxation of Au substrate atoms at the interface, and found that such relaxations do not alter the main findings of the present study in any essential way.

The ARPES data have been measured on *in situ* grown epitaxial films [29] with a Gammadata R4000 spectrometer using monochromatized He I radiation ($h\nu = 21.23$ eV) at low sample temperatures ($T \approx 60$ K). The energy and angle resolution [5] for the presented

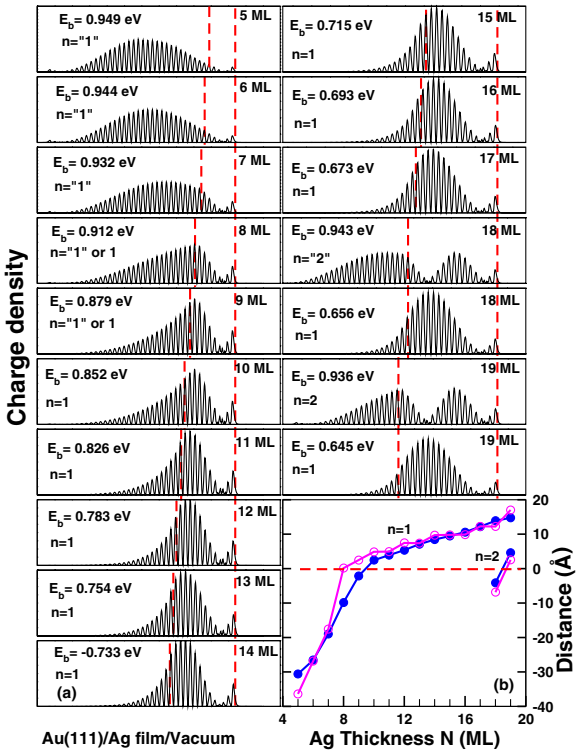

Fig. 1: (Color online) (a) Plane-averaged charge densities along the slab direction of the resonant states (labeled "n") or QWS (labeled n) at $\overline{\Gamma}$ in Ag films grown on an Au(111) substrate. The left and right vertical dashed lines indicate the Au/Ag and Ag/vacuum interfaces, respectively. The binding energies are given with respect to the Fermi level of the Ag/Au(111) system. Note that the calculated upper edge of the valence band of the Au substrate is at 943 meV, as indicated by the solid horizontal lines in figs. 2(a) and (b). (b) The center-of-charge (filled circles) and maximum peak positions (empty circles) of the states in panel (a) relative to the Au/Ag interface.

measurements were $\Delta E \approx 5$ meV and $\Delta\Theta \approx 0.3°$. The Ag film thickness was determined by a quartz micro balance and more precisely from the analysis of the discrete photoemission peak shifts of Shockley and quantum well state due to the layer-by-layer growth of this system. Due to a careful calibration of the preparation procedure we are able to determine the film thickness N with a very high accuracy, which is important for the comparison with the theoretical results.

To illustrate how the resonant states evolve into well-defined QWS as the Ag film thickness, N_{Ag}, increases, we present in fig. 1(a) a series of plane-averaged charge density plots of the eigenstates at $\overline{\Gamma}$ point of the zone center just below the surface states of the overlayer systems, which are the most likely precursors to the QWS trapped in the Ag films. In each panel of fig. 1(a), the left and right vertical dashed lines indicate the Au/Ag and Ag/vacuum interfaces, respectively. Note that all the charge densities appear as an envelope function superimposed on finer oscillations, the latter with the period of the lattice spacing. The charge density of the state is

within the Ag films when $N_{Ag} \geqslant 10$ ML. For $N_{Ag} \leqslant 7$ ML, the state cannot be regarded as the first QWS within the Ag films, not only because the corresponding charge density is mainly distributed in the Au substrate, but also because its binding energy is either lower than or too close to the upper edge of the Au valence band. Note that the calculated upper edge of the valence band of Au substrate is at the binding energy of 0.94 eV, slightly smaller than the experimental value of 1.09 eV, as indicated by the horizontal lines in fig. 2(a) and (b) for the former, and fig. 2(c) for the latter, respectively. In these cases, the strong coupling of the electrons in the Ag film with the Au valence band leads to the formation of a resonant state. The binding energy of the resonant state increases with the Ag film thickness, eventually well within the symmetry gap of the Au substrate, leading to the formation of the first quantum well state. To quantitatively define the onset thickness of each QWS, we introduce two exact criteria, the center-of-charge and the position of the maximum peak for the state, as depicted in fig. 1(b). A QWS is considered to be established when either its center-of-charge, or its maximum peak position, or *both*, lies in the Ag films. The two criteria differ only in the crossover region of 8–9 MLs for the $n = 1$ state. The charge density of the second state below the surface state is also shown in fig. 1(a) for $N_{Ag} = 18$ and 19 ML, corresponding to the thicknesses right before and right after the crossover location of both the center-of-charge and the maximum peak position respectively, as indicated in fig. 1(b).

To gain further insight in the evolution of the QWS, we show the various energy alignments for the cases of freestanding Ag films (fig. 2(a)) and Ag films grown on an Au substrate (fig. 2(b)). In fig. 2(a), the two highest levels are the even and odd surface states, exhibiting the characteristic thickness-dependent splitting of the surface band [30] when the film thickness is less than the decay length of the surface states (12 ML) [31]. The lower subbands are the QWS. Figure 2(a) clearly exhibits a strong thickness dependence of the symmetry gap, which is even larger than the counterpart of the Au substrate when $N_{Ag} < 14$ ML. Therefore, when such a freestanding Ag film is placed on Au(111), the first QWS is likely to be established only when $N_{Ag} > 14$ ML. In contrast, a constant bulklike symmetry gap has been assumed when treating such systems in the literature [8,10,14]. Figure 2(b) illustrates the influence of the substrate. Due to the Fermi level alignment of Ag and Au upon contact, the energy levels in the supported films will shift relative to the freestanding films. One most noticeable change is the reduction of the binding energy of the first state below the surface state at smaller Ag thicknesses. When these binding energies are compared with the location of the upper edge of the Au valence band, one should expect the development of the first and second QWS when $N_{Ag} \geqslant 8$ ML and 19 ML, respectively, consistent with the findings shown in fig. 1(b). Here we also note that the contrasting behavior of QWS in Ag films on different substrates can be reconciled within the same picture. For Ag/Fe(100) and Ag/V(100), the relative symmetry gap for the Δ_1 band is much larger, given by 4.20 eV [17] and 4.74 eV [16], respectively. Therefore, QWS develop at much lower coverage in ultrathin Ag films on Fe(001) and V(001) than in Ag/Au(111) systems [6,13,15,16].

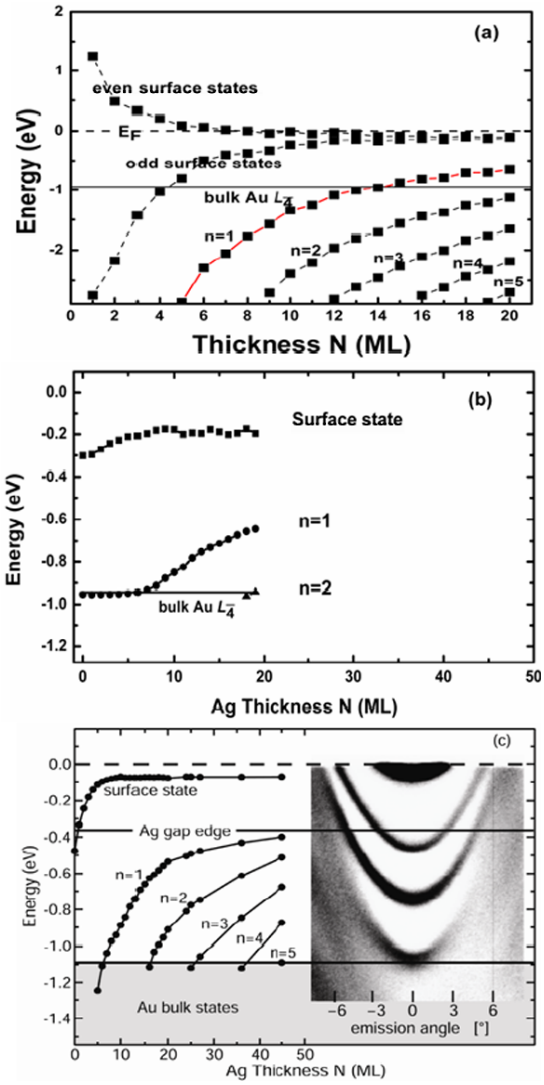

Fig. 2: (Color online) (a) Calculated energy spectra of the subbands at $\overline{\Gamma}$ for freestanding Ag(111) films. The dashed lines connect the eigenstates belonging to the same subbands. The bottom of the symmetry gap along the (111) direction of the Ag films is highlighted by red solid line. (b) Calculated eigenenergies of the surface state and resonant or true QWS for Ag deposited on Au(111). (c) Binding energies of the surface state and QWS for Ag/Au(111) determined by photoemission. The inset in (c) shows a grey-scale plot of the photoemission intensity $I(\theta, E)$ *vs.* emission angle θ and binding energy, including the dispersion of the Shockley state and the first three QWS in a 27 ML Ag film (high intensities appear dark). The gap edge of bulk Ag and bulk Au are denoted by horizontal lines at 370 meV and 1090 meV, respectively. The energy zero is set at the Fermi level for every panel.

Figure 2(c) shows a typical ARPES data set (grey-scale plot on the right side) from a systematic photoemission investigation of the Shockley-type surface state and quantum well states in Ag/Au(111). These high-resolution data together with an accurate determination of the film thickness N allows a detailed comparison with the calculated results above. In particular, the onset thickness of 7 ML for the first QWS ($n=1$), *i.e.* the number of monolayers for which the QWS crosses the gap edge of the substrate at normal emission ($\theta=0$), is very close to the calculated values of 8 to 10 ML for the crossover region (fig. 1(b)) and identical to the calculated binding energy crossover in fig. 2(b). For the second QWS ($n=2$), the experimental onset thickness is 17 ML, also very close to the calculated value of 19 ML from both the energy and exact criteria (fig. 1(b) and fig. 2(b)). We would like to mention that Miller *et al.* observed the first and second QWS at the onset thickness of 10 and 19 ML, respectively.

Here we note that the primary source —on the theory side— for a possible quantitative difference between the calculated and the measured binding energies of the surface and quantum well states lies in the inaccurate determination of the Fermi energy in such DFT studies of systems that have true or symmetry gaps around the Fermi level. This possible uncertainty is one reason why we introduce the two new criteria (the center-of-charge and maximum peak position) to quantitatively determine the onset thicknesses of the QWS, rather than solely relying on the calculated binding energies. The accuracy of the two new criteria is ensured by the underlying charge conservation in all the calculations. More importantly, the three criteria, the binding energy and the two new ones, provide consistent results on the precise *number* of well-defined QWS for all the film thicknesses. In contrast, using the parameterized model with constant bulk band gap energies, Beckmann *et al.* predicted that the QWS in an Ag film grown on Au(111) would set in much earlier (4 and 12 ML for the first and second QWS, respectively) [14].

In addition to the agreement between the theoretical and experimental QWS binding energies (fig. 2(c)), a detailed analysis of the photoemission intensities of the first QWS ($n=1$) confirms nicely the calculated charge distributions given in fig. 1. The photoemission intensity can be calculated by integrating the charge distribution over the depth, weighted with the exponential escape probability characterized by the mean free path (escape depth) λ of the photoelectrons at the respective kinetic energy ($\approx 16\,\mathrm{eV}$ for He I). The best agreement between the measured intensity A_N and the calculated intensity distribution B_N could be obtained by using $\lambda = 4\,\mathrm{ML}$, in perfect agreement with the experimental value of $10\,\text{Å} \equiv 4.23\,\mathrm{ML}$ for Ag(111) [32]. As displayed in fig. 3 the theoretical and the experimental curve are identical within the error bars and show the same maximum position and width. For comparison we show also the result of a simple "particle-in-a-box" model which does not describe the decrease of intensity at low film thicknesses.

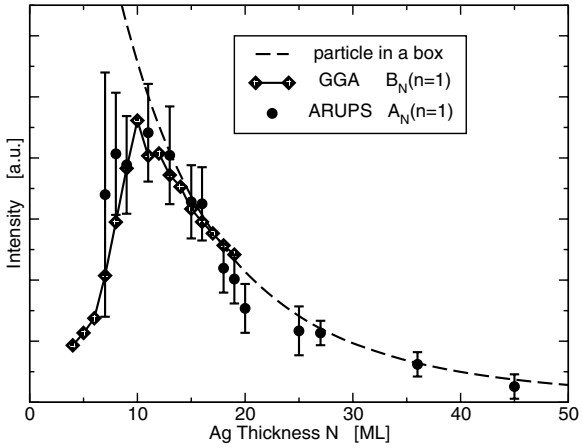

Fig. 3: Comparison of experimental and theoretical photoemission intensity of the first QWS ($n=1$) as a function of the Ag film thickness N. The experimental ARUPS intensity A_N (filled circles) was normalized for each film thickness N to the respective Shockley-state intensity. For the calculation of the theoretical intensities B_N (open diamonds), a photoelectron escape depth of $\lambda = 4$ ML has been used; the dashed line gives the intensity behaviour for a simple one-dimensional "particle-in-a-box".

As discussed before [8,10], if one considers only the misalignment of the symmetry gaps of bulk Ag and Au, no QWS should be formed in Au films grown on an Ag(111) substrate. But based on the present study, the symmetry gap of an ultrathin Ag film can become much larger. Furthermore, given the isovalency and nearly perfect lattice mismatch of Ag and Au, we expect that the synergetic QWS, which are only confined between the two vacuum sides, with negligible influence of the Au/Ag interface, can be established when an Au film is grown on a thin Ag slab. This expectation is confirmed by studying a 5-ML Au film grown on a 5-ML Ag(111) slab, as displayed by the plane-averaged charge density of a representative QWS in fig. 4(a). The results are obtained with the use of a supercell consisting of a 25 Å vacuum layer, plus 5-ML Au supported on a 5-ML Ag slab. For comparison, the corresponding QWS in a 10-ML Ag(111) film is shown in fig. 4(b). The electron density shows negligible perturbation at the Au/Ag interface, and a nearly ideal synergetic QWS spanning across the whole (Au+Ag) system is established [33]. Indeed, recent photoemission studies of the Au/Ag/W(110) systems [11,12] have shown that QWS are characterized by the *total* thickness of the (Au+Ag) overlayers, indicating that such synergetic QWS are robust when the (Au+Ag) overlayers is deposited on a proper substrate.

The above finding, that synergetic QWS can be established in Au films grown on an Ag slab, suggests that potential quantum size effects on chemical rate processes may also exist on such films. In particular, gold is widely used as a catalyst [34], yet in many cases its binding with the supporting materials is not as strong as desired. The

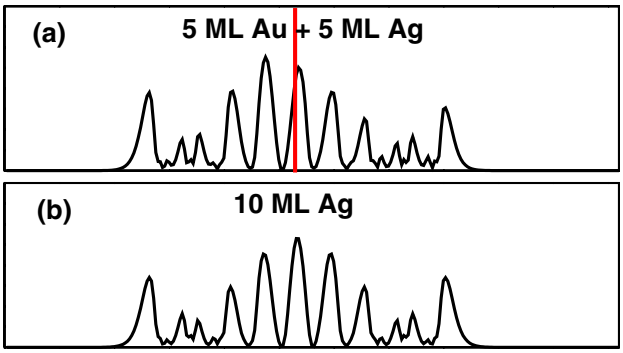

Fig. 4: (a) Plane-averaged charge density of one representative QWS in a 5 ML Au films supported on a 5 ML Ag(111) slab; the vertical line indicates the position of the Au/Ag interface. (b) Plane-averaged charge density of the corresponding QWS in a 10 ML Ag(111) slab.

present finding suggests that one may use an Ag slab as a gluing layer between Au and a substrate, and use the topmost Au layer for catalytic applications. Detailed studies confirming this conjecture for the cases of O and CO adsorption on synergetic (Au+Ag) quantum films will be published elsewhere [35].

Finally, we note that most of the salient features obtained here in DFT studies could be rationalized using a simple one-dimensional (1D) "particle-in-a-box" model with a few fitting parameters. In fact, this was precisely done in a few previous studies of metal film growth on various substrates in the quantum regime [6,8,14,17]. On the other hand, as pointed out above, these earlier treatments unavoidably invoked a constant 1D well depth (the relative gap between bulk bands along certain direction). Besides developing accurate and quantitative descriptions of the specific Ag/Au and Au/Ag systems of interest, our present DFT study also serves another important purpose: It provides important input parameters to future development of simplified 1D models for these and related systems.

In summary, we have carried out a comprehensive combined DFT and high-resolution photoemission study of how a symmetry gap around the Fermi level of ultrathin metal films develops towards its bulk value, using Ag/Au(111) as a prototype example. Contrary to prevailing assumptions, the symmetry gap in ultrathin Ag films can be substantially wider than either the bulk value of Ag or that of the Au(111) substrate. Based on this finding, plus detailed and precise studies of how the resonant states develop into well-defined quantum well states, we have provided quantitative interpretations in these and related systems. Furthermore, we have shown that ideal synergetic QWS can be established in (Ag+Au) thin films with comparable Ag and Au thicknesses, an observation that points to potential tunability of the chemical reactivity on ultrathin catalytic Au films.

* * *

The work at Fudan was partially supported by the NSFC and the Shanghai Project. The work in Tennessee was partially supported by the Division of Materials Sciences and Engineering, Office of Basic Energy Sciences, US Department of Energy, under contract DE-AC05-00OR22725 with Oak Ridge National Laboratory, managed and operated by UT-Battelle, LLC; and by the National Science Foundation under Grant No. DMR-0606485. The work at Würzburg was supported by the Deutsche Forschungsgemeinschaft (RE1469/4-3). Furthermore, we thank Prof. M. Y. Chou for a critical reading of the manuscript.

REFERENCES

[1] Li J., Li X., Zhai H. J. and Wang L. S., *Science*, **299** (2003) 864.
[2] Sattler K., *in Handbook of Thin Films Materials*, edited by Nalwa H. S., Vol. **5** (Academic Press) 2001, chapt. 2, p. 61.
[3] Echenique P. M. and Pendry J. B., *Prog. Surf. Sci.*, **32** (1989) 111.
[4] Höfer U. *et al.*, *Science*, **277** (1997) 1480.
[5] Reinert F. *et al.*, *Phys. Rev. B*, **63** (2001) 115415.
[6] Milun M., Pervan P. and Woodruff D. P., *Rep. Prog. Phys.*, **65** (2002) 99.
[7] Qiu Z. Q. and Smith N. V., *J. Phys: Condens. Matter*, **14** (2002) R169.
[8] Chiang T.-C., *Surf. Sci. Rep.*, **39** (2000) 181.
[9] Zhang Z. Y., *Surf. Sci.*, **571** (2004) 1.
[10] Miller T., Samsavar A., Franklin G. E. and Chiang T.-C., *Phy. Rev. Lett.*, **61** (1988) 1404.
[11] Shikin A. M. *et al.*, *Phys. Rev. B*, **62** (2000) R2303.
[12] Vyalikh D. V. *et al.*, *Surf. Sci.*, **540** (2003) L638.
[13] Wei C. M. and Chou M. Y., *Phys. Rev. B*, **68** (2003) 125406.
[14] Beckmann A., Klaua M. and Meinel K., *Phys. Rev. B*, **48** (1993) 1844.
[15] Paggel J. J., Miller T. and Chiang T.-C., *Science*, **283** (1999) 1709.
[16] Ernst A., Henk J., Lüders M., Szotek Z. and Temmerman W. M., *Phys. Rev. B*, **66** (2002) 165435.
[17] Smith N. V., Brookes N. B., Chang Y. and Johnson P. D., *Phys. Rev. B*, **49** (1994) 332.
[18] Ogando E., Zabala N., Chulkov E. V. and Puska M. J., *Phys. Rev. B*, **71** (2005) 205401.
[19] Evans D. A., Alonso M., Cimino R. and Horn K., *Phys. Rev. Lett.*, **70** (1993) 3483.
[20] Smith A. R., Chao K. J., Niu Q. and Shih C. K., *Science*, **273** (1996) 226.
[21] Yeh V., Berbil-Bautista L., Wang C. Z., Ho K. M. and Tringides M. C., *Phys. Rev. Lett.*, **85** (2000) 5158.
[22] Gavioli L., Kimberlin K. R., Tringides M. C., Wendelken J. F. and Zhang Z. Y., *Phys. Rev. Lett.*, **82** (1999) 129.
[23] Yu D. K., Scheffler M. and Persson M., *Phys. Rev. B*, **74** (2006) 113401.

[24] Fournee V. *et al.*, *Phys. Rev. Lett.*, **95** (2005) 155504.
[25] Kresse G. and Furthmüller J., *Comput. Mater. Sci.*, **6** (1994) 15.
[26] Vanderbilt D., *Phys. Rev. B*, **41** (1990) 7892; Kresse G. and Hafner J., *J. Phys. Condens. Matter*, **6** (1994) 8245.
[27] Perdew J. P. and Wang Y., *Phys. Rev. B*, **45** (1992) 6671.
[28] Monkhorst H. J. and Pack J. D., *Phys. Rev. B*, **13** (1976) 5188.
[29] Cercellier H. *et al.*, *Phys. Rev. B*, **73** (2006) 195413.
[30] Schiller F., Keyling R., Chulkov E. V. and Ortega J. E., *Phys. Rev. Lett.*, **95** (2005) 126402.
[31] Hsieh T. C. and Chiang T. C., *Surf. Sci.*, **166** (1986) 554.
[32] Hansen E. D., Miller T. and Chiang T. C., *Phys. Rev. B*, **55** (1997) 554.
[33] Mcmahon W. E., Mueller M. A., Miller T. and Chiang T. C., *Phys. Rev. B*, **49** (1994) 10426.
[34] Bond G. C. *et al.* (Editor), *Catalysis by Gold*, Vol. **6** (Imperial College Press) 2006.
[35] Huang L. *et al.*, unpublished.